Nano Energy 32 (2017) 263–270

Contents lists available at ScienceDirect

Nano Energy

journal homepage: www.elsevier.com/locate/nanoen

On the ability of Förster resonance energy transfer to enhance luminescent solar concentrator efficiency

Clemens Tummeltshammer[a], Mark Portnoi[a], Serena A. Mitchell[b], An-Tser Lee[b], Anthony J. Kenyon[a], Alethea B. Tabor[b], Ioannis Papakonstantinou[a,*]

[a] Department of Electronic and Electrical Engineering, University College London, London WC1E 7JE, United Kingdom
[b] Department of Chemistry, University College London, London WC1H 0AJ, United Kingdom

ARTICLE INFO

Keywords:
Luminescent solar concentrators
Förster resonance energy transfer
Quantum dots
Organic dye molecules
Solar energy

ABSTRACT

Developing means to reduce the cost of solar energy is vital to curb our carbon footprint over the upcoming decades. A luminescent solar concentrator (LSC) is a potential solution as it provides light concentration without any tracking device and can be readily integrated into the built environment. In this study we report on an advanced LSC design that employs quantum dots as absorption fluorophores and organic dye molecules as emission fluorophores. By linking the two types of fluorophores to each other, energy is transferred efficiently via Förster resonance energy transfer (FRET) from the quantum dot to the dye molecule. This novel method makes use of the quantum dot's spectrally wide absorption profile and the higher quantum yield of the dye. We show that our design can overcome the losses normally incurred due to a low quantum yield emitter by transferring the absorbed energy to a linked fluorophore with a higher quantum yield. Our experimental measurements show FRET can enhance the optical efficiency of a LSC by at least 24.7%. The maximum theoretical efficiency has been investigated by ray-tracing and has been found to be 75.1%; this represents a relative improvement of even 215.5% compared to a LSC doped with quantum dots only (23.8%), showing the great potential of our concept. Our design will initiate interest in fluorophores which have not been considered for LSC applications thus far because of their low quantum yield or small Stokes shift.

1. Introduction

Luminescent solar concentrators (LSCs) were invented in the late 70s to reduce the cost of solar energy by concentrating the incident sunlight, [1–3]. A flat, transparent host is doped with fluorophores which absorb the incoming photons and emit them again at a longer wavelength. Through total internal reflection, photons are trapped within the host to reach the thin side surfaces which have solar cells adhered to. This reduces the need for costly solar cell material and additionally makes expensive tracking systems redundant as not only direct but also diffuse light is absorbed by LSCs.

Despite their great potential, LSCs have struggled to make a strong impact on solar energy due to the following shortcomings (see also Fig. 1a): (1) fluorophores will lose some of the absorbed energy to heat due to a *non-unity quantum yield*, (2) depending on the direction of emission, the photons could be lost via the *escape cone*, (3) commonly used fluorophores have a *spectrally narrow absorption band*, and (4) *overlapping absorption and emission spectra* cause emitted photons to be re-absorbed exacerbating shortcomings (1) and (2). An additional concern for LSC researchers is the photostability of the fluorophores to make them suitable for long-term outdoor applications, [4–7].

To absorb a wider part of the solar spectrum and increase the photon's wavelength shift, it was suggested to mix multiple types of fluorophores at high concentrations and induce Förster resonance energy transfer (FRET) [8–12]. The high concentration is needed to ensure that the different types of fluorophores are in close proximity for FRET to occur. Highly concentrated fluorophores are prone to aggregation though, which can alter their properties such as lowering their quantum yield. The dense packing of fluorophores can be avoided by linking the donor and acceptor fluorophores; examples of linked fluorophores include phycobilisomes or dendritic energy cascades, [13,14]. Another approach involves rare earth ion based hybrids which have the benefit of negligible re-absorption, [15].

Dye molecules can be aligned homeotropically to improve the trapping efficiency and thus reduce escape cone losses, [16–20]. Such an alignment will generally limit the absorption of the incoming light as the dye's dipole moment and the electric field vector of the incident light will be close to orthogonal to each other. To circumvent the low

* Corresponding author.
E-mail address: i.papakonstantinou@ucl.ac.uk (I. Papakonstantinou).

http://dx.doi.org/10.1016/j.nanoen.2016.11.058
Received 4 July 2016; Received in revised form 1 November 2016; Accepted 29 November 2016
Available online 18 December 2016

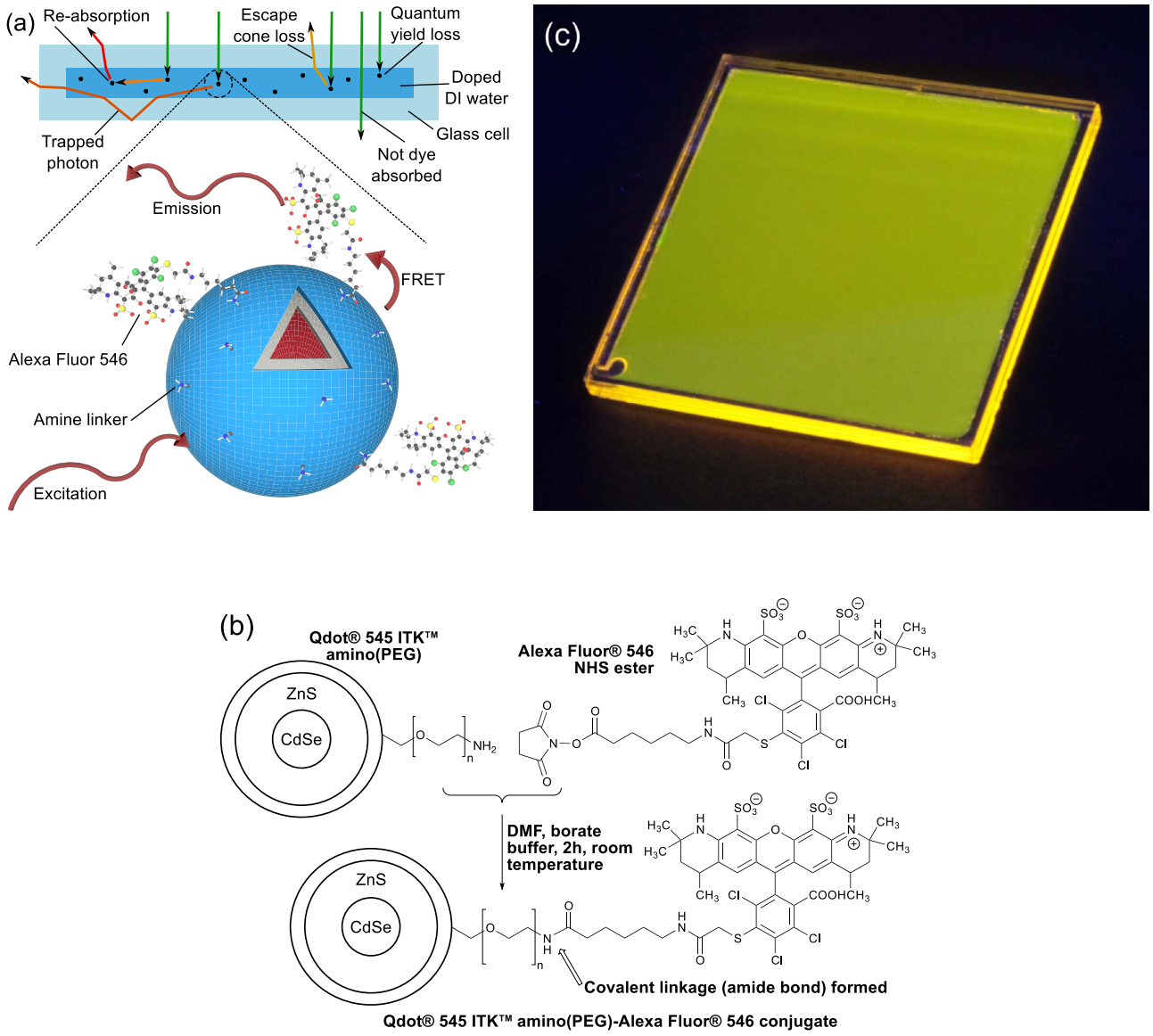

Fig. 1. (a) The concept of our design: a LSC glass cell holds DI water which is doped with a quantum dot/dye molecule conjugate. Absorbed incoming light is either re-emitted, trapped and guided towards the side surfaces or lost due to a non-unity quantum yield or via the escape cone. The close-up depicts the conjugate; the quantum dot (Qdots 545) consists of a core (CdSe), a shell (ZnS) and an amphiphilic polymer coating with amine linkers attached to it. Dye molecules (Alexa Fluor 546) are attached to the quantum dot using their NHS-ester linker. Incident radiation is absorbed by the quantum dot and transferred via FRET to the dye molecule which relaxes radiatively. (b) A chemistry reaction scheme for the conjugation of quantum dots and dye molecules. (c) Our LSC glass cell filled with the conjugate under UV radiation.

absorption of a homeotropically aligned dye molecule, a second fluorophore can be utilized to serve as a donor or absorption fluorophore, [17,21–24]. If the donor is in the proximity of the dye molecule, the absorbed energy can be transferred to the dye via FRET. The donor should preferably have a spectrally wide absorption spectrum; quantum dots generally fulfill this requirement but suffer from a lower quantum yield, in particular commercially available ones [25–28]. It was shown though, that a lower quantum yield is not a hindrance to be a suitable donor in a fluorophore pair due to the efficiency of FRET as long as the emission fluorophore has a sufficiently high quantum yield, [23].

Despite the quantum dot's spectrally wide absorption spectrum, the emission spectrum is generally quite narrow; by varying the size of the quantum dot the emission spectrum can be tuned towards the absorption spectrum of any acceptor to maximize FRET. Also, quantum dots (10–100 ns) commonly have longer exciton decay lifetimes than organic fluorophores (1–10 ns) which will make it easier for the FRET decay rate to compete with the small radiative and non-radiative decay rates of the quantum dot [29,30]. The phase coherence loss, also denoted dephasing, which has been observed with quantum dots, is another beneficial property of donor fluorophores for LSC applications [31,32]. Dephasing enables the decoupling between the direction of the incident electric field and the induced dipole moment in the donor; this way more efficient energy transfer will occur from the donor to the homeotropically aligned acceptor, [21]. Quantum dots also benefit from having a high photostability compared to organic dye molecules, [29]. However, it was shown that the organic dye molecule chosen for this study, part of the Alexa Fluor series, has superior photostability compared to other organic dye molecules making it suitable for LSC applications, [33].

Motivated by these findings, we have conjugated quantum dots with dye molecules to induce FRET between them. We have chosen quantum dots as the absorption fluorophores/donors and dye molecules as emission fluorophores/acceptors; the quantum dots have a spectrally wide absorption spectrum and the dye molecule have a higher quantum yield. As a proof-of-concept, we have developed a LSC

doped with conjugated dye molecules and quantum dots which entails a LSC efficiency improvement of 24.7% compared to using quantum dots only. A LSC doped with unlinked quantum dots and dye molecules performs even worse than the quantum dots by themselves due to the lack of FRET and the re-absorption by the dye molecules. Experiments with a solar simulator and a commercial solar cell attached to the sides of the LSC, also showed considerable improvement in optical efficiency under AM1.5g illumination for the conjugate sample compared with the rest of the samples. The concept and our prototype LSC are shown in Fig. 1.

We are, to the best of our knowledge, the first to show experimentally to which extent the linking of inorganic to organic fluorophores enhances the performance of a LSC. It is shown that, thanks to FRET, fluorophores with lower quantum yield and small Stokes shift can still be viable candidates for LSCs as absorption fluorophores; our findings will also support research in other areas where quantum dots are used as donors such as the bioanalysis of nucleic acids, immunoassays, pH sensing, or dye-sensitized solar cells, [34–40].

2. Results and discussion

2.1. Optimal ratio between dyes and quantum dots

Qdot 545 ITK amino(PEG) quantum dots (Qdots) have an amphiphilic surface coating, to which is attached an amine-derivatized PEG, allowing it to react effectively with succinimidyl derivatives, [41]. We therefore reacted the Qdots with the N-hydroxysuccinimidyl (NHS) ester of the Alexa Fluor 546 dye (AFDye), thus creating a covalent linkage between the Qdots and the AFDyes, as shown in Fig. 1b.

Multiple AFDye-NHS ester molecules can be linked to the surface of one Qdot functionalized with amine linkers. A higher degree of labeling (DOL - see also Degree of labeling section in Supporting Information) will improve the energy transfer from the quantum dot to a dye molecule; at the same time re-absorption by the dye molecules will increase and interactions between the dye molecules attached to the same quantum dot become more probable. To determine the optimal DOL, different initial AFDyes:Qdots ratios are investigated which are shown in Table 1. The chosen initial ratios are (A) 10:1, (B) 20:1, (C) 25:1, (D) 60:1 and (E) 120:1. As described in Section 4, the actual DOL is determined using absorbance measurements. Lifetime measurements will yield the transfer efficiency and determining the fluorescence of each sample will show if attaching dye molecules to the quantum dots does enhance the emission.

Fig. 2 shows the absorbance spectrum for the conjugate A. The sum of the Qdot and dye absorbances nicely resembles the absorbance of the conjugate; thus the linking changes the absorbance of the individual fluorophores only slightly. The actual degrees of labeling are on average equal to 7.3:1, 10.7:1, 13.1:1, 27.9:1 and 40.4:1 for samples A, B, C, D, and E, respectively. The average separation between the QDots and AFDyes was found by FRET theory to be r=7.6 ± 0.4 nm for all DOLs (see Distance between donor and acceptor in the Supporting Information), which is in excellent agreement with the hydrodynamic radius of the QDot nanocrystal (r=8 nm). This indicates that FRET is the predominant mechanism for energy exchange between the quantum dot and the dyes.

Table 1
Different AFDyes:Qdots ratios investigated in this work and their respective DOL and transfer efficiency.

Sample	Initial ratio	DOL	FRET
A	10:1	7.3:1	59.9%
B	20:1	10.7:1	73.8%
C	25:1	13.1:1	80.1%
D	60:1	27.9:1	90.3%
E	120:1	40.4:1	93.9%

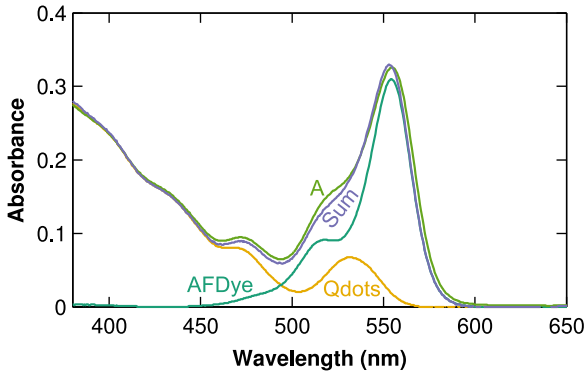

Fig. 2. The absorbance spectra of the Qdots, the AFDyes and sample A. For comparison the sum of the Qdots and the AFDyes is shown.

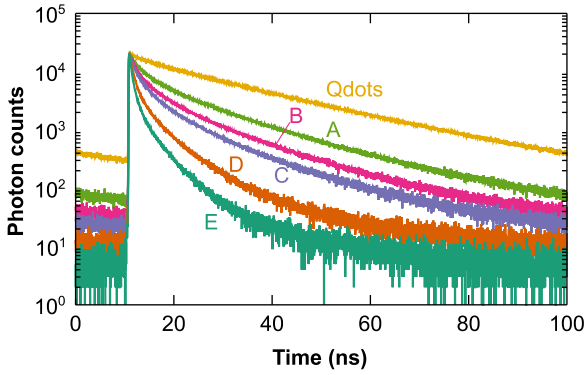

Fig. 3. Time-resolved fluorescence lifetime measurements of the Qdots and the conjugates using an excitation wavelength of 405 nm.

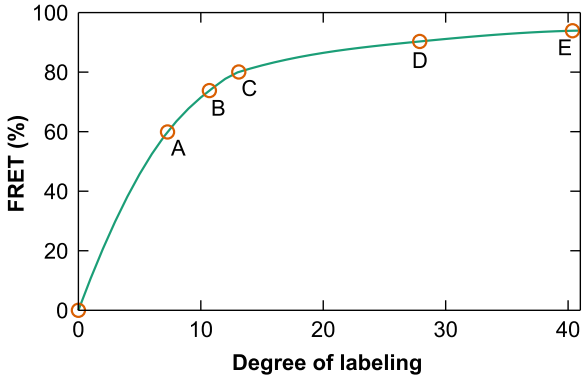

Fig. 4. FRET as a function of DOL. The degree of labeling will be lower than the starting ratio as some dyes will not have linked to the quantum dots. Circles show experimental measurements, while the line is an interpolation of the measurements to guide the eyes of the reader.

Lifetime measurements are taken at 535 nm to only register emission from the Qdots as emission of the AFDyes is negligible below about 550 nm. The resulting lifetime curves are shown in Fig. 3 for all conjugates and one sample with only Qdots. Additionally, the lifetime of the AFDye is determined to be 4.1 ns (detection wavelength of 569 nm) which matches company data, [42]. If more dyes are connected to one Qdot, more energy absorbed by the Qdot will be transferred to the attached dye molecules. This will reduce the measured lifetime of the emission coming directly from the Qdot. The resulting energy transfer efficiency is depicted in Fig. 4. The FRET values are shown as a function of DOL. The energy transfer efficiency increases at first quite strongly with DOL, but after a DOL of around 13:1 every additional dye molecule does not add much to the transfer

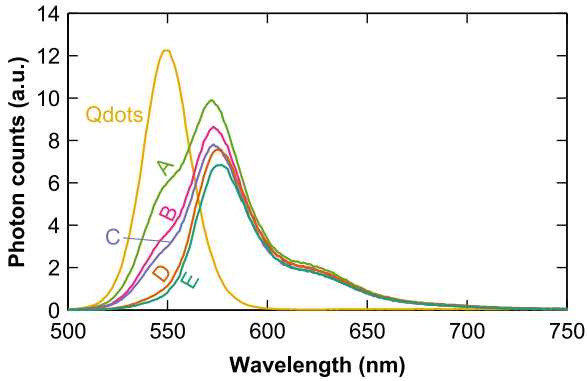

Fig. 5. Emission measurements of the Qdots and the different conjugates using a fluorescence spectrometer. The excitation wavelength is equal to 405 nm and the graphs take into account the absorbance of each sample at this wavelength.

efficiency. Every time a dye molecule is added to the nanocrystal, it will reduce the lifetime of the quantum dot. As a result, it becomes increasingly difficult for the decay rate representing the energy transfer from the quantum dot to the newly added dye to compete with the decay rates of the nanocrystal. At the same time more dye molecules will aggravate re-absorption; thus a balance has to be found between higher FRET and lower re-absorption.

A fluorescence spectrometer is used to determine which DOL depicts the strongest fluorescence and how it compares to a sample with only quantum dots. Fig. 5 depicts the emission profiles for the investigated samples with an excitation source of 405 nm. While care is taken during the fabrication of the samples to ensure the same concentration of quantum dots among the samples, slight variations will occur. To take this into account, the depicted emission profiles are the measured fluorescence divided by the absorbance of each sample at 405 nm. The emission by the quantum dots is strongly quenched due to FRET, in particular for sample E. There is also a red-shift that increases with the DOL as re-absorption by the dye molecules increases. Even though sample A depicted a lower FRET value than the other ratios, it is the strongest emitter as re-absorption is weaker. Also, for a higher DOL dye molecules linked to the same Qdot could interact with each other which will create additional decay channels and potentially affect their quantum yield. For sample E the integrated photon count is 12.9% lower compared to the Qdots by themselves due to the aforementioned reasons. Sample A, though, emits 49.6% more photons than the quantum dots by themselves as a result of FRET. Some of the photons that would be lost due to the lower quantum yield of the Qdots are instead transferred to the dye molecules and emitted. For the comparisons above the emission spectra are integrated over the entire wavelength range.

2.2. Internal optical efficiency results

As described previously, the performance of a LSC can be determined with the help of an integrating sphere, [43]. The *internal optical efficiency* is the probability that a photon reaches the side surfaces after a photon is first absorbed by a fluorophore. In contrast, the *optical efficiency* takes into account every photon that reaches the front surface of the LSC. Since the absorption levels of the samples investigated in this work are the same, a sample with a better internal optical efficiency will also have a superior optical efficiency.

Based on the results above, sample A with an initial ratio of 10:1 is the most promising candidate for a prototype LSC with linked quantum dots and dye molecules. As a proof-of-concept, the conjugate is injected into the LSC glass cell to determine its internal optical efficiency compared to non-linked samples.

For the following measurements four different samples are injected into the LSC glass cell: (1) Qdots only, (2) Qdots and AFDyes which are not linked, (3) Qdots and AFDyes conjugated using an initial ratio of 10:1, and (4) AFDyes only. All samples have the same concentration of Qdots (2.5×10^{-6} mol L^{-1}) and/or dyes (1.8×10^{-5} mol L^{-1}). As mentioned in Section 4, the dyes were kept in DI water to become non-reactive for the unlinked sample. However, a few dyes remained reactive and conjugated to the quantum dot resulting in a transfer efficiency of 14.7%; unlike the conjugate sample, the unlinked one is not centrifuged though which means that the majority of dyes in the unlinked sample are not attached to any Qdot. The conjugate sample with an initial ratio of 10:1 made for the following experiments turned out to have a slightly lower FRET efficiency of 51.5% than the one in the previous measurements (59.9%). Potential reasons include that the conjugation was performed using larger volumes and that some of the dyes in the AFDye/DMF mixture have become non-reactive between the preparation of the two different 10:1 samples.

With the help of the integrating sphere, the quantum yield of the AFDye is determined to be 79% which matches the company data very accurately, [42,44]. Measurements using the integrating sphere indicate though that the quantum yield of the Qdots is somewhat lower than reported by the company. The quantum yield is verified to be 42% by additionally comparing it to the quantum yield of Coumarin 6 in Ethanol (see Quantum yield of QDots section in Supporting Information), [45,46]. The lower value could be due to the different solvent and pH level, [47].

Fig. 6 shows the total emission (i.e. escaping through all six surfaces) of the four samples inside the integrating sphere. The dye only sample emits weaker than the other samples due to the low absorption. The dye only sample absorbs less than 1%, while the other samples absorb about 13.5% at the incoming wavelength of 450 nm. The excitation wavelength of 450 nm is chosen to limit direct absorption by the dye molecules; this ensures that any potential enhancement is due to FRET. The conjugate sample again outperforms the Qdots sample; the increase in total emitted photons (24.1%) is not as pronounced as with the fluorescence spectrometer. Firstly, the FRET efficiency is lower for this sample resulting in more photons being lost by the lower quantum yield of the quantum dots. Secondly, the emission is trapped within the LSC glass cell and therefore re-absorption will be more dominant than in the fluorescence spectrometer. This will affect the conjugate sample stronger as the dye concentration is about seven times higher than the quantum dot concentration. Since the dye sample has the same concentration as the conjugate one and the former only absorbs 1%, it is evident that only a small share of the conjugate emission is due to direct dye excitation. The conjugate also emits 13.3% more photons than the unlinked sample, proving that linking the quantum dots and dye molecules is essential to boost the LSC performance.

The performance enhancement becomes even clearer when con-

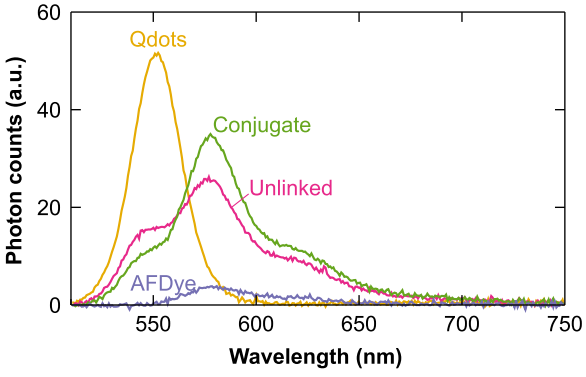

Fig. 6. Measured emission of the samples enclosed in the LSC glass cell within the integrating sphere. The four samples shown are the Qdots (orange), the conjugated sample (green), a sample with quantum dots and dye molecules that are not linked (pink) and an AFDye sample (purple). The emission escaping through the front, the back and all four side surfaces is measured.

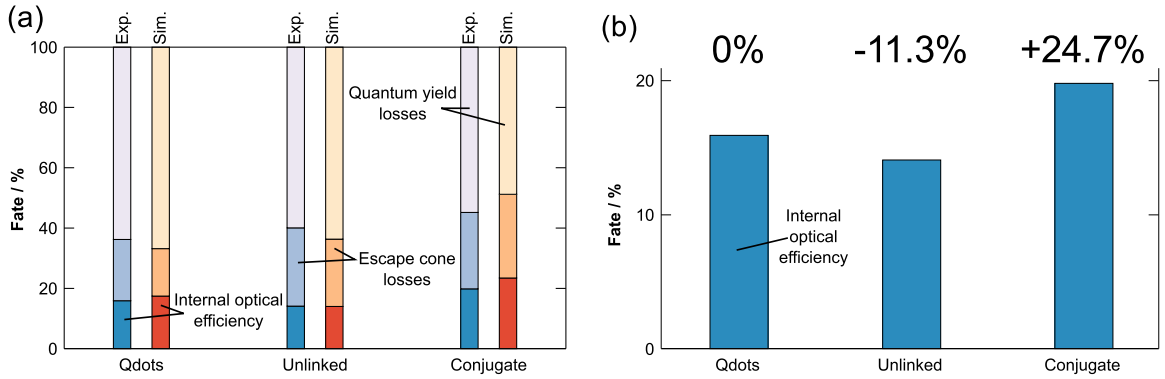

Fig. 7. The experimental (blue) and simulation (red) LSC metrics results of the different samples. Qdots is the sample doped with quantum dots only, Unlinked is the sample with quantum dots and dye molecules that are not linked and Conjugate denotes the linked sample. (b) Depicts a magnification of the experimental efficiency results. Also shown is the relative improvement of the experimentally measured internal optical efficiency compared to the Qdots sample.

sidering the LSC metrics which are shown in Fig. 7 and derived from two independent measurements. The experimentally measured internal optical efficiency, escape cone losses and non-unity quantum yield losses are compared to ray-tracing simulations, a modeling technique commonly used for LSCs, which we have extended to include FRET, [48,23,43]. The internal optical efficiencies of the three samples are 15.9% ± 0.1%, 14.1% ± 0.1% and 19.8% ± 0.2% for the Qdots, the unlinked and the conjugate samples, respectively. This represents a relative improvement of 24.7% ± 1.2% from the Qdots sample to the conjugate one. This is due to the non-unity quantum yield losses dropping from 63.8% ± 0.1% to 54.8% ± 0.3%. Photons that would be lost due to the low quantum yield of the quantum dots are now transferred via FRET to the dye molecule which has a higher quantum yield. This was achieved using a dye molecule with a quantum yield of 79% in this proof-of-concept prototype; the improvement would be even stronger for acceptors with a higher quantum yield.

To demonstrate that the enhancement is due to the linkage, we also compare an unlinked sample with the Qdots one. The unlinked sample, which has the same concentration of quantum dots and dye molecules as the conjugate, has a 11.3% ± 0.2% lower internal optical efficiency in relative terms than the quantum dots only sample. The same number of photons are lost due to the lower quantum yield of the quantum dots; re-emitted photons are then additionally re-absorbed by the present independent dye molecules which increases escape cone losses and non-unity quantum yield losses. The decrease is not that strong since the sample still showed some FRET as not all dye molecules have become non-reactive. Assuming no linkage at all between the Qdots and the dye molecules our ray tracer predicts an internal optical efficiency of only 10.9% and non-unity quantum yield losses of 69.0%. This represents a relative internal optical efficiency decline of 31.7% and 45.3% compared to the Qdots and the conjugate samples, respectively.

2.3. Solar simulator results

In the previous section, we used a single excitation wavelength to furnish the contribution of the FRET process to the performance enhancement of the conjugate sample. Herein, we investigate the optical efficiency of our LSCs when exposed to the entire solar spectrum. For the following experiments the efficiency of the LSCs to the AM1.5g spectrum is determined, with the help of a commercial solar-cell attached to their side. Multiplying the efficiency with the geometrical gain, yields the concentration factor, [49], which is used as the figure of merit for comparison between the different LSC samples. Concentration factors achieved previously in the literature are in the ranges of 0.05–0.54 for organic molecules and quantum dots in organic solvents [28,50], 0.10–0.90 for cylindrical LSCs doped with Rhodamine 6G or Eu^{3+} [50], 0.271 for cylindrically shaped LSCs doped with PbS quantum dots [51,52], CdSe/ZnS (0.08) and PbS (0.18) in liquid solutions [53], and 1.91 for CdSe core/multishell quantum dots in PLMA, [27].

IV measurements were performed with a commercial solar simulator system (LS0905, LOT Oriel) for four LSC designs (conjugate 10:1, unlinked, AFDyes only, Qdots only). In this particular experiment, a glass cell with area 20 mm×20 mm was used. The lamp of the system was calibrated to provide an irradiance of 1 sun (1000 W/m^2) at the surface of the LSC, while the AM1.5g solar spectrum was emulated in the experiments by an appropriate bandpass filter (LSZ189). A polycrystalline silicon (*p*-Si) solar cell (RVFM-34038, Rapid Online) of active area 19 mm×3 mm, was attached to one side of the LSCs under test. The geometrical gain achieved was thus, G=7 in all cases. The efficiency of the p-Si solar cell was measured with the solar simulator

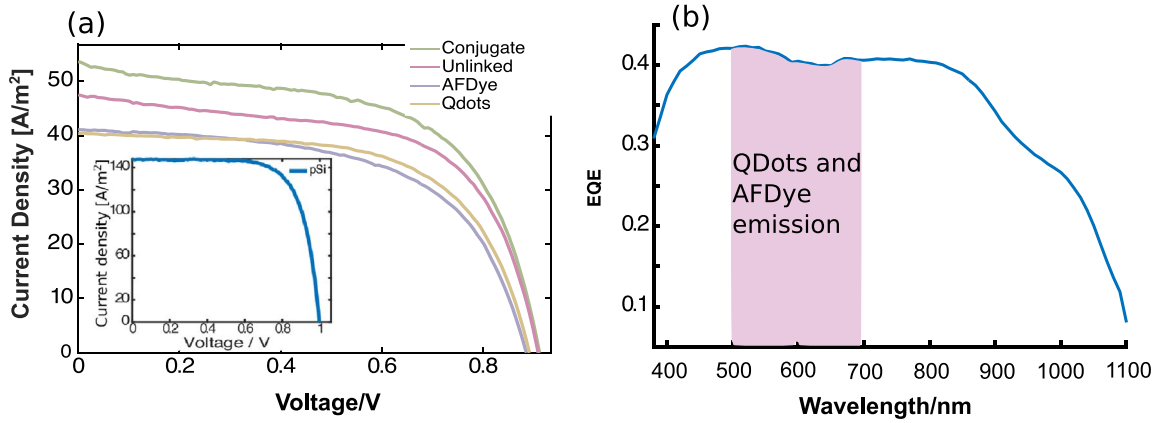

Fig. 8. (a) IV curves for the four LSCs characterised in this work. Inset: IV curve of p-Si solar cell. (b) EQE for p-Si solar cell. Shaded area: Spectral region of Qdot and AFDye emission.

Table 2
Efficiency of various LSCs investigated in this work.

LSC	Efficiency	Concentration
AFDyes	2.11%	0.163
Qdots	2.24%	0.173
Unlinked	2.62%	0.203
Conjugate	2.87%	0.222

and was found to be 10.6%. While commercially available solar cells with better efficiency exist, the particular solar cell was chosen as its external quantum efficiency was relatively flat (~40%) over the emission spectra of both the Qdots and the AFDyes (see Fig. 8b); this facilitates comparison between the different LSCs. Index matching fluid (Cargille, n=1.56) was applied at the interface between the LSC and the p-Si cell to suppress reflections. A diffuse aluminum reflector was mounted at the bottom of the LSC to increase the absorbance of the device. The results in Fig. 8a demonstrate a noticeable increase to both the short-circuit current and the open-circuit voltage of the conjugated LSC compared with the three other LSCs. The efficiency of the conjugated LSC is 2.87% (see Table 2) normalized with respect to the AM1.5g spectrum, which corresponds to a concentration factor of 0.222. These values represent a relative increase of 36%, 28% and 10% compared with the AFDyes only, the Qdots only and the unlinked LSCs, respectively. Unlike for the internal optical efficiency measurements (see Fig. 7), the unlinked sample performs better than the Qdots sample. This is due to the spectrally wider absorption of the unlinked sample which offsets its lower internal optical efficiency. However, the difference in efficiency between conjugated and unlinked LSCs will increase with the geometrical gain G, as longer optical paths will lead to more pronounced reabsorption losses that mostly affect the unlinked sample, as was discussed in the previous section.

2.4. Ray tracing results

We have shown in the previous sections using a proof-of-concept prototype, that FRET can strongly improve the efficiency of a LSC. If fluorophores and hosts with better optical properties are chosen, even higher efficiencies can be achieved. Here, we use ray tracing to determine the potential internal optical efficiency using our method of linking quantum dots to dye molecules. Assuming a homogeneous slab with a refractive index of 1.49 as host, a transfer efficiency of 93.9% (the maximum one achieved in this work), a DOL of unity, a quantum yield of 95% for the dye, and a homeotropically aligned dye, an internal optical efficiency of 75.1% is achieved (see Monte-Carlo ray tracing section in Supporting Information for further details). This represents a 215.5% improvement compared to a quantum dots only LSC (23.8%) in a homogeneous slab with a refractive index of 1.49. The same design would achieve an AM1.5g normalized optical efficiency of 10.9% due to the wide spectral absorption, effective energy transfer and minimized escape cone losses. To reach such a high efficiency level the fluorophore concentration needs to be increased to around 2.5×10^{-5} mol L^{-1} to enhance the initial absorption.

3. Conclusion

We have shown experimentally for the very first time that LSC performance enhancement can be achieved by linking quantum dots to dye molecules. Our optimum conjugate sample outperformed the quantum dots sample by 24.7% due to 51.5% of the absorbed energy being transferred to the dye molecule via FRET; the dye emits the photons more efficiently than the quantum dot as it has a higher quantum yield. Experiments with a solar simulator and a commercially available p-Si solar cell revealed that the efficiency of our LSC reaches 2.87% with only one solar cell attached. Our materials have also shown low degradation under UV irradiation (365 nm central wavelength, 1058 W m^{-2}) for 5 h which eludes that this system shows potential resilience to solar exposure (see UV degradation section in Supporting Information). This work is only a proof-of-concept though; in fact, we have shown using ray-tracing simulations that internal optical efficiencies of up to 75.1% can be reached with our advanced design which results in an improvement of 215.5% compared to a LSC doped with quantum dots only. This requires additionally a high quantum yield dye and fluorophore alignment; the next challenge is to align the emission fluorophore which has been demonstrated previously [21,22,24].

To further improve the performance of our design, a high FRET should be achieved with fewer dye molecules. One potential solution are alloyed quantum dots that have varying optical properties based on their composition rather than their diameter and are available in smaller sizes [54–56]. This would reduce the center-to-center distance between the nanocrystal and the dyes and thus improve the transfer efficiency. Attaching fewer dyes would reduce re-absorption by the fluorophores and potential interactions between dyes attached to the same quantum dot. To maximize the power generated by the LSC system, customised solar cells attuned to the emission of the dye molecules are required as well.

Our work demonstrates the great potential of FRET for LSCs by using an absorption and an emission fluorophore. This way fluorophores with a lower quantum yield and a small Stokes shift but a spectrally wide absorption spectrum can still be utilized in LSCs. A small Stokes shift would neither be a hindrance as the photons undergo a strong red-shift due to FRET. This means that researchers would get access to a large numbers of fluorophores that would otherwise not be suitable.

4. Methods

Qdot 545 ITK amino(PEG) quantum dots (Qdots) and Alexa Fluor 546 NHS ester dyes (AFDyes) were purchased from Life Technologies. Anhydrous dimethylformamide (DMF) was purchased from Sigma-Aldrich and deionized water was bought from VWR.

Conjugation: AFDyes were dissolved in anhydrous DMF at a concentration of 1 mg/100 µl (8.6 mM). Qdots were supplied in borate buffer (50 nm) at a concentration of 8.6 µM. The two solutions were mixed together in appropriate amounts in order to give a range of initial AFDyes:Qdots ratios (10:1, 20:1, 25:1, 60:1 and 120:1). Thus, for an initial AFDyes:Qdots molar ratio of 10:1, 1 µl of AFDye solution was mixed with 100 µl of Qdots solution. The mixture was then vortexed at 1000 rpm for 2 h at room temperature in the dark. Unbound AFDye molecules were then removed using a centrifugal filter (50 kDa MWCO, Millipore) at 3000 rpm. The AFDye molecules have a molecular weight of 1,159.6 g mol^{-1} and, if unbound, are therefore not retained by the filter. Only AFDye molecules with a covalent linkage to the Qdots will remain within the solution. The AFDyes-Qdots conjugates were then resuspended in deionized water.

Control sample: The AFDyes/DMF solution was mixed with deionized water and stored in the dark at room temperature for one week to allow the NHS ester to hydrolyze. After this the unreactive dye was mixed with the appropriate ratio of Qdots solution to give a control sample in which the AFDyes and the Qdots are not linked.

Optical characterization: The degree of labeling (DOL) is a measure of how many dye molecules are linked on average to one single quantum dot. The DOL can be determined with the help of the absorbance profile of the sample as described in the Supporting Information. To measure the absorbance a UV–vis spectrophotometer (Shimadzu) was used. Lifetime and emission measurements were performed using a fluorescence spectrometer (Edinburgh Instruments) at an excitation wavelength of 405 nm. With the help of the lifetime results the transfer efficiency can be calculated [47]: $\text{FRET} = 1 - \frac{\tau_C}{\tau_Q}$ where τ_C and τ_Q are the amplitude-weighted lifetimes

of the conjugate and the quantum dots, respectively. The amplitude-weighted lifetime of a multiexponential decay is given by $\tau = \frac{\sum A_i \tau_i}{\sum A_i}$ with A_i being the amplitudes of the different decays τ_i. The internal optical efficiency, escape cone losses and non-unity quantum yield losses of a LSC are measured using our own novel method which we described elsewhere [43].

LSC glass cell: As the Qdots with amine linker are hydrophilic, DI water is used as solvent for all measurements. To determine the potential of the fluorophores as LSC dopants, the fluorophores dissolved in DI water are injected into a glass cell, a method commonly used for LSCs [28,53]. The size of the LSC glass cell is 40×40×2.7 mm^3 with a glass thickness of 1 mm. The LSC glass cell filled with conjugated Qdots and AFDyes is shown in Fig. 1c. Due to the lower refractive index of water compared to commonly used solid host materials such as Poly(methyl methacrylate) (PMMA), the trapping efficiency and thus the LSC efficiency will be lower. However, the main target of this work is to show the potential improvement by linking fluorophores for which the LSC glass cell is perfectly suited.

Acknowledgement

This work was supported by the European Union Framework Programme 7 (FP7) via a Marie-Curie Career Integration Grant, Project no. 293567. We acknowledge financial support from UCL BEAMS School via a Ph.D. Impact Award and from the UK Engineering and Physical Sciences Research Council (EPSRC grant no. EP/K015354/1). We also acknowledge Alaric Taylor for helping with the fabrication of the glass cell and for general discussions.

Appendix A. Supplementary data

Supplementary data associated with this article can be found in the online version at http://dx.doi.org/10.1016/j.nanoen.2016.11.058.

References

[1] W.H. Weber, J. Lambe, Luminescent greenhouse collector for solar radiation, Appl. Opt. 15 (1976) (2299–300).
[2] A. Goetzberger, W. Greube, Solar energy conversion with fluorescent collectors, Appl. Phys. 14 (1977) 123–139.
[3] I. Papakonstantinou, C. Tummeltshammer, Fundamental limits of concentration in luminescent solar concentrators revised the effect of reabsorption and nonunity quantum yield, Optica 2 (2015) 841–849.
[4] I. Baumberg, O. Berezin, A. Drabkin, B. Gorelik, L. Kogan, M. Voskobojnik, M. Zaidman, Effect of polymer matrix on photo-stability of photo-luminescent dyes in multi-layer polymeric structures, Polym. Degrad. Stab. 73 (2001) 403–410.
[5] S.F.H. Correia, P.P. Lima, P.S. André, M.R.S. Ferreira, L.A.D. Carlos, High-efficiency luminescent solar concentrators for flexible waveguiding photovoltaics, Sol. Energy Mater. Sol. Cells 138 (2015) 51–57.
[6] G. Griffini, L. Brambilla, M. Levi, M. Del Zoppo, S. Turri, Photo-degradation of a perylene-based organic luminescent solar concentrator molecular aspects and device implications, Sol. Energy Mater. Sol. Cells 111 (2013) 41–48.
[7] G. Griffini, M. Levi, S. Turri, Novel high-durability luminescent solar concentrators based on fluoropolymer coatings, Prog. Org. Coat. 77 (2014) 528–536.
[8] B.A. Swartz, T. Cole, A.H. Zewail, Photon trapping and energy transfer in multiple-dye plastic matrices an efficient solar-energy concentrator, Opt. Lett. 1 (1977) 73–75.
[9] S.T. Bailey, G.E. Lokey, M.S. Hanes, J.D.M. Shearer, J.B. McLafferty, G.T. Beaumont, T.T. Baseler, J.M. Layhue, D.R. Broussard, Y.-Z. Zhang, B.P. Wittmershaus, Optimized excitation energy transfer in a three-dye luminescent solar concentrator, Sol. Energy Mater. Sol. Cells 91 (2007) 67–75.
[10] M.J. Currie, J.K. Mapel, T.D. Heidel, S. Goffri, M.A. Baldo, High-efficiency organic solar concentrators for photovoltaics, Science 321 (2008) 226–228.
[11] J.L. Banal, K.P. Ghiggino, W.W.H. Wong, Efficient light harvesting of a luminescent solar concentrator using excitation energy transfer from an aggregation-induced emitter, Phys. Chem. Chem. Phys. 16 (2014) 25358–25363.
[12] B. Balaban, S. Doshay, M. Osborn, Y. Rodriguez, S.A. Carter, The role of FRET in solar concentrator efficiency and color tunability, J. Lumin. 146 (2014) 256–262.
[13] C.L. Mulder, L. Theogarajan, M. Currie, J.K. Mapel, M.A. Baldo, M. Vaughn, P. Willard, B.D. Bruce, M.W. Moss, C.E. McLain, J.P. Morseman, Luminescent solar concentrators employing phycobilisomes, Adv. Mater. 21 (2009) 3181–3185.
[14] O. Altan Bozdemir, S. Erbas-Cakmak, O.O. Ekiz, A. Dana, E.U. Akkaya, Towards unimolecular luminescent solar concentrators bodipy-based dendritic energy-transfer cascade with panchromatic absorption and monochromatized emission, Angew. Chem. -Int. Ed. 50 (2011) (10907–12).
[15] J. Graffion, X. Cattoën, M.Wong Chi. Man, V.R. Fernandes, P.S. André, R.A.S. Ferreira, L.D. Carlos, Modulating the photoluminescence of bridged silsesquioxanes incorporating Eu 3+-complexed n,*n*-diureido-2,2-bipyridine isomers application for luminescent solar concentrators, Chem. Mater. 23 (2011) 4773–4782.
[16] P.P.C. Verbunt, A. Kaiser, K. Hermans, C.W.M. Bastiaansen, D.J. Broer, M.G. Debije, Controlling light emission in luminescent solar concentrators through use of dye molecules aligned in a planar manner by liquid crystals, Adv. Funct. Mater. 19 (2009) 2714–2719.
[17] R.W. MacQueen, Y.Y. Cheng, R.G.C.R. Clady, T.W. Schmidt, Towards an aligned luminophore solar concentrator, Opt. Express 18 (2010) A161–A166.
[18] M.G. Debije, Solar energy collectors with tunable transmission, Adv. Funct. Mater. 20 (2010) (1498–502).
[19] C.L. Mulder, P.D. Reusswig, A.M. Velázquez, H. Kim, C. Rotschild, M.A. Baldo, Dye alignment in luminescent solar concentrators I. vertical alignment for improved waveguide coupling, Opt. Express 18 (2010) A79–A90.
[20] C.L. Mulder, P.D. Reusswig, A.P. Beyler, H. Kim, C. Rotschild, M.A. Baldo, Dye alignment in luminescent solar concentrators II. horizontal alignment for energy harvesting in linear polarizers, Opt. Express 18 (2010) A91–A99.
[21] R.W. MacQueen, T.W. Schmidt, Molecular polarization switching for improved light coupling in luminescent solar concentrators, J. Phys. Chem. Lett. 4 (2013) 2874–2879.
[22] J. ter Schiphorst, A.M. Kendhale, M.G. Debije, C. Menelaou, L.M. Herz, A.P.H.J. Schenning, Dichroic perylene bisimide triad displaying energy transfer in switchable luminescent solar concentrators, Chem. Mater. 26 (2014) 3876–3878.
[23] C. Tummeltshammer, A. Taylor, A.J. Kenyon, I. Papakonstantinou, Homeotropic alignment and foerster resonance energy transfer the way to a brighter luminescent solar concentrator, J. Appl. Phys. 116 (2014) 173103.
[24] C. Menelaou, J.T. Schiphorst, A.M. Kendhale, P. Parkinson, M.G. Debije, A.P.H.J. Schenning, L.M. Herz, Rapid energy transfer enabling control of emission polarization in perylene bisimide donor-acceptor triads, J. Phys. Chem. Lett. (2015) (1170–6).
[25] O.E. Semonin, J.C. Johnson, J.M. Luther, A.G. Midgett, A.J. Nozik, M.C. Beard, Absolute photoluminescence quantum yields of IR-26 Dye, PbS, and PbSe quantum dots, J. Phys. Chem. Lett. 1 (2010) 2445–2450.
[26] Y. Wu, G.P. Lopez, L.A. Sklar, T. Buranda, Spectroscopic characterization of streptavidin functionalized quantum dots, Anal. Biochem. 364 (2007) 193–203.
[27] J. Bomm, A. Büchtemann, A.J. Chatten, R. Bose, D.J. Farrell, N.L.A. Chan, Y. Xiao, L.H. Slooff, T. Meyer, A. Meyer, W.G.J.H.M. van Sark, R. Koole, Fabrication and full characterization of state-of-the-art quantum dot luminescent solar concentrators, Sol. Energy Mater. Sol. Cells 95 (2011) 2087–2094.
[28] V. Sholin, J.D. Olson, S.A. Carter, Semiconducting polymers and quantum dots in luminescent solar concentrators for solar energy harvesting, J. Appl. Phys. 101 (2007) 123114.
[29] U. Resch-Genger, M. Grabolle, S. Cavaliere-Jaricot, R. Nitschke, T. Nann, Quantum dots versus organic dyes as fluorescent labels, Nat. Methods 5 (2008) 763–775.
[30] A.R. Clapp, I.L. Medintz, J.M. Mauro, B.R. Fisher, M.G. Bawendi, H. Mattoussi, Fluorescence resonance energy transfer between quantum dot donors and dye-labeled protein acceptors, J. Am. Chem. Soc. 126 (2004) 301–310.
[31] U. Woggon, M. Portuné, C. Klingshirn, H. Giessen, B. Fluegel, G. Mohs, N. Peyghambarian, Dephasing processes in II-VI quantum dots, Phys. Status Solidi B 188 (1995) 221–227.
[32] F. Grosse, E.A. Muljarov, R. Zimmermann, Phonons in Quantum Dots and Their Role in Exciton Dephasing, in: D. Bimberg (Ed.), Semiconductor Nanostructures, Springer, Berlin Heidelberg, 2008, pp. 165–87.
[33] N. Panchuk-Voloshina, R.P. Haugland, J. Bishop-Stewart, M.K. Bhalgat, P.J. Millard, F. Mao, W.Y. Leung, R.P. Haugland, Alexa dyes, a series of new fluorescent dyes that yield exceptionally bright, photostable conjugates, J. Histochem. Cytochem. 47 (1999) 1179–1188.
[34] C.-Y. Zhang, H.-C. Yeh, M.T. Kuroki, T.-H. Wang, Single-quantum-dot-based DNA nanosensor, Nat. Mater. 4 (2005) 826–831.
[35] W.R. Algar, U.J. Krull, Towards multi-colour strategies for the detection of oligonucleotide hybridization using quantum dots as energy donors in fluorescence resonance energy transfer (FRET), Anal. Chim. Acta 581 (2007) 193–201.
[36] W.R. Algar, U.J. Krull, Quantum dots as donors in fluorescence resonance energy transfer for the bioanalysis of nucleic acids, proteins, and other biological molecules, Anal. Bioanal. Chem. 391 (2008) (1609–18).
[37] Q. Wei, M. Lee, X. Yu, E.K. Lee, G.H. Seong, J. Choo, Y.W. Cho, Development of an open sandwich fluoroimmunoassay based on fluorescence resonance energy transfer, Anal. Biochem. 358 (2006) 31–37.
[38] P.T. Snee, R.C. Somers, G. Nair, J.P. Zimmer, M.G. Bawendi, D.G. Nocera, A ratiometric CdSe/ZnS nanocrystal pH sensor, J. Am. Chem. Soc. 128 (2006) 13320–13321.
[39] I.L. Medintz, H. Mattoussi, Quantum dot-based resonance energy transfer and its growing application in biology, Phys. Chem. Chem. Phys. 11 (2009) 17–45.
[40] S. Itzhakov, S. Buhbut, E. Tauber, T. Geiger, A. Zaban, D. Oron, Design principles of FRET-Based dye-sensitized solar cells with buried quantum dot donors, Adv. Energy Mater. 1 (2011) 626–633.
[41] K. Takayama, A. Tadokoro, S. Pujals, I. Nakase, E. Giralt, S. Futaki, Novel system to achieve one-pot modification of cargo molecules with oligoarginine vectors for intracellular delivery, Bioconjug. Chem. 20 (2009) 249–257.
[42] Thermo Fisher Scientific, Quantum yield of Alexa Fluor 546, ⟨https://www.thermofisher.com/uk/en/home/references/molecular-probes-the-handbook/tables/fluorescence-quantum-yields-and-lifetimes-for-alexa-fluor-dyes.html⟩, 2015.

[43] C. Tummeltshammer, A. Taylor, A.J. Kenyon, I. Papakonstantinou, Losses in luminescent solar concentrators unveiled, Sol. Energy Mater. Sol. Cells 144 (2016) 40–47.
[44] J.C. de Mello, H.F. Wittmann, R.H. Friend, An improved experimental determination of external photoluminescence quantum efficiency, Adv. Mater. 9 (1997) 230–232.
[45] A.T.R. Williams, S.A. Winfield, J.N. Miller, Relative fluorescence quantum yields using a computer-controlled luminescence spectrometer, Analyst 108 (1983) 1067–1071.
[46] G.A. Reynolds, K.H. Drexhage, New coumarin dyes with rigidized structure for flashlamp-pumped dye lasers, Opt. Commun. 13 (1975) 222–225.
[47] J.R. Lakowicz, Principles of Fluorescence Spectroscopy, Springer, New York, NY, USA, 2006.
[48] C. Tummeltshammer, M.S. Brown, A. Taylor, A.J. Kenyon, I. Papakonstantinou, Efficiency and loss mechanisms of plasmonic luminescent solar concentrators, Opt. Express 21 (2013) (A735–49).
[49] M. Carrascosa, S. Unamuno, F. Agullo-Lopez, Monte carlo simulation of the performance of PMMA luminescent solar collectors, Appl. Opt. 22 (1983) 3236.
[50] S.F.H. Correia, P.P. Lima, E. Pecoraro, S.J.L. Ribeiro, P.S. Andre, R.A.S. Ferreira, L.D. Carlos, Scale up the collection area of luminescent solar concentrators towards metre-length flexible waveguiding photovoltaics, Prog. Photovolt. Res. Appl. 24 (2016) 1178–1193.
[51] R.H. Inman, G.V. Shcherbatyuk, D. Medvedko, A. Gopinathan, S. Ghosh, Cylindrical luminescent solar concentrators with near-infrared quantum dots, Opt. Express 19 (2011) (24308–13).
[52] S.F.H. Correia, V. De Zea Bermudez, S.J.L. Ribeiro, P.S. André, R.A.S. Ferreira, L.D. Carlos, Luminescent solar concentrators challenges for lanthanide-based organic-inorganic hybrid materials, J. Mater. Chem. A 2 (2014) 5580–5596.
[53] G.V. Shcherbatyuk, R.H. Inman, C. Wang, R. Winston, S. Ghosh, Viability of using near infrared PbS quantum dots as active materials in luminescent solar concentrators, Appl. Phys. Lett. 96 (2010) 191901.
[54] N.P. Gurusinghe, N.N. Hewa-Kasakarage, M. Zamkov, Composition-tunable properties of CdSxTe1-x Alloy nanocrystals, J. Phys. Chem. C 112 (2008) (12795–800).
[55] A.M. Smith, S. Nie, Next-generation quantum dots, Nat. Biotechnol. 27 (2009) 732–733.
[56] J. Feng, H. Zhu, X. Wang, X. Yang, Composition-dependent fluorescence emission of ternary Cd-In-S alloyed quantum dots, Chem. Commun. 48 (2012) 5452–5454.